

Impact of the tip radius on the lateral resolution in piezoresponse force microscopy

Tobias Jungk,* Ákos Hoffmann, and Elisabeth Soergel
*Institute of Physics, University of Bonn,
 Wegelerstraße 8, 53115 Bonn, Germany*

(Dated: October 15, 2018)

We present a quantitative investigation of the impact of tip radius as well as sample type and thickness on the lateral resolution in piezoresponse force microscopy (PFM) investigating bulk single crystals. The observed linear dependence of the width of the domain wall on the tip radius as well as the independence of the lateral resolution on the specific crystal-type are validated by a simple theoretical model. Using a Ti-Pt-coated tip with a nominal radius of 15 nm the so far highest lateral resolution in bulk crystals of only 17 nm was obtained.

PACS numbers: 68.37.Ps, 77.84.-s, 77.65.-j

Ferroelectrics attract increasing attention due to their applicability, e.g., for electrically controlled optical elements [1], for efficient frequency-doubling [2, 3], for photonic crystals [4], or for non-volatile memories with an otherwise un-reached data-storage density [5]. The size of the domain structures required for those applications varies from a few microns down to some nanometers. The smaller the domains are the more the properties of the domain walls become important. Generally the width of the domain walls is expected to be a few crystal lattice cells [6, 7, 8]. Measuring the birefringence with scanning near-field microscopy in LiTaO₃, however, showed a distortion of the crystal over a width of 3 μm across the domain boundary [9]. Detecting the Raman modes with a confocal defect-luminescence microscope, an influence of the domain wall in LiNbO₃ further than 1 μm into the surrounding material was observed [10]. On the other hand, high-resolution transmission electron microscopy yielded a domain wall width in PbTiO₃ of < 2.5 nm [11] and with scanning nonlinear dielectric microscopy, a width of only 0.5 nm in ultra-thin PZT films was determined [12].

In the past ten years, piezoresponse force microscopy (PFM) has become a very common technique for domain imaging mainly due to its high lateral resolution without any need for specific sample preparation. In brief, for PFM a scanning force microscope is operated in contact mode with an alternating voltage applied to the tip. In ferroelectric samples this voltage causes thickness changes via the converse piezoelectric effect [13] and therefore vibrations of the surface which lead to oscillations of the cantilever that can be read out with a lock-in amplifier [14, 15].

In this contribution, we present a study of the influence of the tip radius on the PFM imaging of 180° ferroelectric domain walls in bulk single crystals. Therefore we determined the width W of domain walls when imaged

by PFM on LiNbO₃ crystals for tips of different radii. We also compared W for different types of crystals using one unique tip. Furthermore, a series of measurements was carried out with LiNbO₃ of different sample thicknesses. Finally we present a simple analytical model that explains the observed dependencies of the domain wall W on the tip radius, the crystal thickness and type of sample.

The experiments were carried out with two different scanning force microscopes (Topometrix Explorer from Veeco and SMENA from NT-MDT). Both systems were modified to allow application of voltages to the tip in order to enable PFM measurements. The alternating voltage ($U_{\text{tip}} = 10 \text{ V}_{\text{pp}}$, 30 – 60 kHz) was applied to the tip and the backside of the samples was grounded. To obtain reliable data for the width W we readout the X -signal of the lock-in amplifier (in the following denoted as PFM signal). The recorded data were thus unaffected by the background inherent to PFM measurements [16] which can lead to a presumed broadening of the width W [17].

We used a series of different tips with radii varying from 10 – 90 nm, classified in Tab. I. All tips were made out of highly n-doped silicon and conductively coated with different materials. The spring constants ranging from 3 to 70 N/m. The tip with the smallest radius ($r = 10 \text{ nm}$) makes an exception since it was uncoated. Due to oxidization the outer few nanometers of the surface are modified to non-conductive SiO₂. As a consequence, the mechanical and the electrical tip do not coincide any more; the SiO₂-layer acts as a dielectric gap between tip and sample.

The experiments for determining the dependence of the width W on the tip radius r were performed with periodically poled (period length $\Lambda = 30 \mu\text{m}$) congruently melting 500 μm thick LiNbO₃ crystals (PPLN). For the measurements of W on the sample thickness t we used the same LiNbO₃ samples, mechanically thinned by polishing to the thickness wanted (15 – 1000 μm). The thinnest sample (0.9 μm) was a stoichiometric LiNbO₃ crystal. Here the domains were generated with the help of the tip by applying a voltage of 20 V for 10 min.

*Electronic address: jungk@uni-bonn.de

TABLE I: Specifications of the different tips utilized for the measurements.

Label	Manufacturer	Model	Tip radius [nm]	Coating
A	NT-MDT ^a	NSG11	10	–
B	Veeco ^b	OSCM-PT	15	Ti-Pt
C	Veeco ^b	SCM-PIT	20	Pt-Ir
D	MikroMash ^c	NSC35	35	Ti-Pt
E	MikroMash ^c	NSC35	50	Cr-Au
F	NT-MDT ^a	DCP11	50–70	diamond
G	MikroMash ^c	NSC35	90	Co-Cr

^awww.ntmdt.ru

^bwww.veeco.com

^cwww.spmtips.com

We also measured a series of samples different from LiNbO₃ as listed in Tab. II. Those samples had thicknesses of 0.5 – 2 mm and were either periodically poled (KTiOPO₄ and LiNbO₃) or had arbitrary domain patterns (BaTiO₃, KNbO₃, LiTaO₃ and Sr_{0.61}Ba_{0.39}Nb₂O₆).

Calculating the spatial resolution achievable with PFM requires the exact electric field distribution underneath the tip and the electromechanical answer of the material. The latter is given by the dielectric constants as well as the elastic and piezoelectric tensors, respectively. This complex problem is most suitable for the finite element method (FEM), where all material constants can be included thus yielding quantitative results [18]. A detailed study on domain wall width imaged by PFM including FEM-calculations has recently been undergone [19]. In this contribution, we propose a much simplified approach to the problem of lateral resolution in PFM. This model is not capable of giving the amplitude of the measured PFM signals because we performed some normalization in order to facilitate the calculations. The model can, however, give a quantitative prediction of the width W as a function of the tip radius r and the sample thickness t .

In a first step the problem was simplified by approximating the spherical apex of the tip with radius r by a point charge at the distance r above the sample surface. We further assumed the sample to be isotropic with an effective dielectric constant $\epsilon_{\text{eff}} = \sqrt{\epsilon_r \epsilon_z}$, ϵ_z being the dielectric constant in z -direction and ϵ_r the radial one perpendicular to z . The electric field distribution underneath the tip is then given by [20]:

$$E_z(x, y, z) = \frac{q}{\epsilon_{\text{eff}}} \left\{ \frac{z+r}{[x^2 + y^2 + (z+r)^2]^{3/2}} + \frac{z-r-2t}{[x^2 + y^2 + (z-2t-r)^2]^{3/2}} \right\}. \quad (1)$$

Next we define E_{max} as the maximum electric field underneath the tip apex inside the sample (at $x = y = z = 0$). E_{max} will be used to normalize the electric field strength.

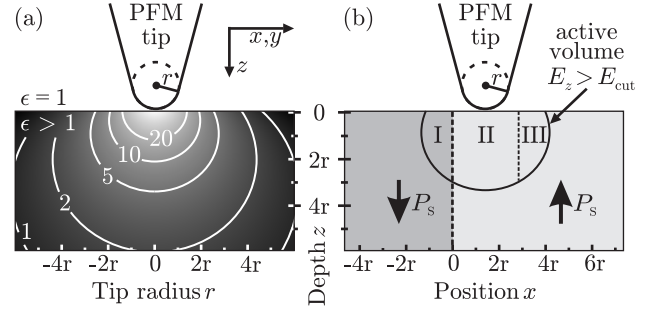


FIG. 1: (a) Electrical field distribution E_z underneath a tip of radius r calculated with Eq. 1 for a sample of infinite thickness. The white lines indicate the shells where the electric field has decayed to the indicated %-value of the maximum electric field E_{max} present underneath the tip apex. (b) Schematics of the analytical model with the tip in the vicinity of a domain wall. The active volume where $E_z > E_{\text{cut}} \approx 0.05 E_{\text{max}}$ underneath the tip covers both domains. The contributions of part I and III cancel out each other. The resulting surface deformation is thus determined by part II only.

Furthermore, we scale all lengths with the tip radius r . The problem has thus become dimensionless. Figure 1(a) shows the electric field distribution E_z inside a sample of infinite thickness. It can be seen, that at a depth of twice the tip radius r , the electric field has decayed to almost 10% of its initial value E_{max} .

Figure 1(b) illustrates the analytical model used for the simulation of the lateral resolution of PFM depending on the tip radius and the sample thickness. First we define an *active volume* inside of which the electric field has decreased to a value E_{cut} which has to be identified later by fitting the experimental data. Beyond the active volume we set $E_z = 0$. The resulting piezomechanical deformation is calculated by integrating the contributions of the sample within the active volume:

$$\Delta z(x) = d_{33} z \int_{-E_{\text{cut}}}^{E_{\text{cut}}} \int_0^{E_{\text{cut}}} E_z(x, y, z) dE_y dE_z. \quad (2)$$

As can be seen in Fig. 1(b) the contributions of region I and III to the emerging piezomechanical deformation cancel out each other. For the simulation of the PFM signal when scanning across a domain wall, the active volume was subdivided into approx. 10^9 cubic elements. In order to determine E_{cut} the experimental data was fitted with the calculated slopes of the PFM signal across the domain wall. The best fits were obtained for $E_{\text{cut}} = 0.92 E_{\text{max}}$ for all tip radii. Note that the main assumption made for the simulation consists in the stiffness of the crystal, i.e., within a length of some microns the crystal parts can not deform independently. The strength of clamping in bulk samples has been demonstrated by other experiments [21].

In order to deduce the domain wall width W from the experimental data we normalized the PFM signals to an amplitude of 1 and fitted the data with a modified hy-

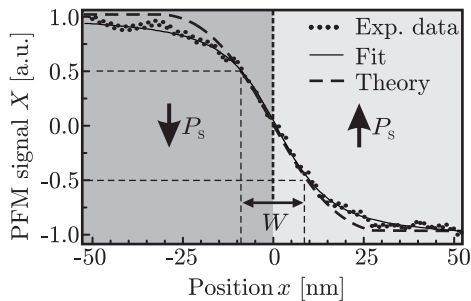


FIG. 2: Measured PFM signal line scan (●) across a 180° domain wall in LiNbO_3 recorded with a tip of type B ($r = 15 \text{ nm}$). The domain wall width W is determined fitting the data using Eq. 3. For comparison, a line scan is shown that was calculated with the theoretical model for a tip with a radius of 15 nm .

perbolic tangent

$$X(x) = A \tanh\left(\frac{x}{w}\right) + B \arctan\left(\frac{x}{w}\right) \quad (3)$$

where A , B and w are used as free parameters. Note that this function is only used to determine the width W but has no direct physical meaning. We then applied a 25% – 75% criterion on the scan lines of the PFM signal which corresponds to the full width at half maximum of the PFM amplitude if no PFM background is present [17]. Figure 2 shows an example for a $r = 15 \text{ nm}$ tip on a LiNbO_3 sample. The measurement (dotted line) is fitted according to Eq. 3 (solid line). For comparison the slope of the PFM signal calculated with the analytical model is also depicted (dashed line). As can be seen, the error determining W using Eq. 3 is minimal that is why we do not show any error bars in the subsequent graphs.

Processing the data in the above described manner, we extracted the data for W as a function of the tip radius as shown in Fig. 3. The straight line results from our analytical model. The excellent agreement between measurement and model is striking and strongly sustains the model to give reasonable estimates on W . Implicit to our model, an atomically sharp domain wall is thus also sustained by the PFM measurements. Note that with tip B a width of only 17 nm was measured, the smallest value recorded with PFM in bulk materials so far. This has to be compared with a recent publication, where a lowest limit for W of 65 nm in LiNbO_3 was estimated [22]. This value as well as our currently highest resolution is by no means a fundamental limit of the material itself but by the available tip sizes and imaging parameters. It is furthermore evidently seen that the non-coated tip A shows a substantially reduced lateral resolution ($W \approx 50 \text{ nm}$) than pretended by its tip radius of only 10 nm . This, however, is exactly what can be expected from an surface oxide layer: the conductive part of the tip being at a distance of some nanometers from the sample surface, separated by the dielectric SiO_2 -layer generates an less localized electrical field inside the crystal, thus the reduced spatial resolution.

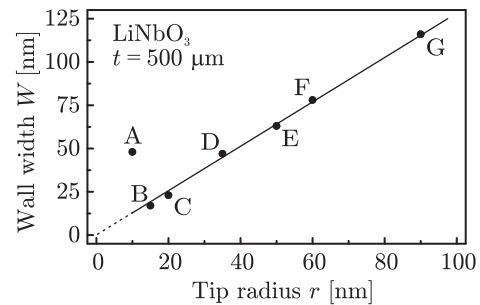


FIG. 3: Measured domain wall width W as a function of the nominal tip radius r (Tab. I). The straight line was calculated using the analytical model presented in this contribution. Note that despite its smaller radius, the uncoated tip A shows an inferior lateral resolution.

In a further series of experiments we determined W as a function of the sample thickness t varying the latter by three orders of magnitude from $0.9 - 1000 \mu\text{m}$ (Fig. 4). We used tips of type D with a nominal radius $r = 35 \text{ nm}$. The accuracy and durability of the tips were controlled by measuring a standard $500 \mu\text{m}$ thick PPLN sample before and after each data acquisition with a sample of modified thickness. From Fig. 4 no change of the width W within the thicknesses range of the samples could be observed. This, however, is consistent with our theoretical model where the electric field distribution E_z is found to be independent on the sample thickness t for $t > 15r$. In the case of tip D with a nominal radius of $r = 35 \text{ nm}$ the electric field E_z is thus the same for samples with thicknesses $> 500 \text{ nm}$.

Finally we compared W for different crystals using tips of type B and D (Tab. II). We again checked the reliability of the recorded data by always recording comparative measurements with a standard PPLN sample. All samples show the same width W for a specific tip of radius $r = 15 \text{ nm}$ or $r = 35 \text{ nm}$ within an error of $\pm 1 \text{ nm}$, although their dielectric anisotropy $\gamma = \sqrt{\epsilon_z/\epsilon_r}$ differ as listed in Tab. I. This can be understood if we calculate the electrical field e. g. with the method of image charges where we place the charge q at $(0, 0, -r)$. In contrast

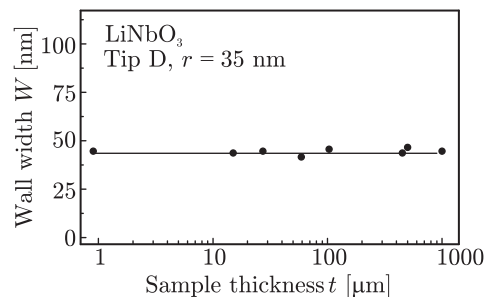


FIG. 4: Measured domain wall width W as a function of sample thickness t . The straight line is the result from the analytical model.

TABLE II: Domain wall width W measured for different samples with tips of type B ($r = 15$ nm) and D ($r = 35$ nm). c-LiNbO₃: congruently melting and s-LiNbO₃: stoichiometric lithium niobate respectively, SBN: Sr_{0.61}Ba_{0.39}Nb₂O₆.

Sample	Domain wall width W [nm]		Dielectric anisotropy $\gamma = \sqrt{\varepsilon_z/\varepsilon_r}$
	$r = 15$ nm	$r = 35$ nm	
BaTiO ₃	19	46	0.18
KNbO ₃	18	45	0.34
KTiOPO ₄	17	46	0.86
LiTaO ₃	18	45	0.89
c-LiNbO ₃	17	46	0.58
s-LiNbO ₃	17	45	0.58
Mg:LiNbO ₃	18	47	0.58
SBN	18	48	1.30

to the case of an infinite isotropic half-plane, characterized by a single dielectric constant, we need two image charges q' at $(0, 0, r)$ and \tilde{q} at $(0, 0, \tilde{r})$ to account for the dielectric anisotropy given by ε_z and ε_r . The potential distribution above the surface is identical to the isotropic case but inside the crystal it is given by

$$\varphi(x, y, z) = \frac{\tilde{q}}{\sqrt{\varepsilon_r^2 \varepsilon_z}} \frac{1}{\sqrt{(x^2 + y^2)/\varepsilon_r + (z - \tilde{r})^2/\varepsilon_z}}. \quad (4)$$

The only way to satisfy the boundary conditions at the surface $(x, y, 0)$ is to set $\tilde{r} = \gamma r$ which leads to

$$E_z(x, y, z) = \frac{2q\gamma}{1 + \varepsilon_{\text{eff}}} \frac{z + r}{[x^2 + y^2 + (z + r)^2]^{3/2}}. \quad (5)$$

From this equation we can clearly see that the dielectric anisotropy does not affect the shape of the electrical field distribution but only the field strength.

To summarize, we have analyzed the impact of the tip radius and the sample thickness on the domain wall width W observed with piezoresponse force microscopy. We introduced an analytical model which explains the experimental data: a linear dependency of W on the tip radius as well as no dependency of W on the sample thickness as long as the sample is thicker than 15-times the tip radius. The model assuming an infinite sharp domain wall is perfectly consistent with the experimental data. Furthermore we carried out a series of measurements for different kind of single crystals. Even though their material parameters differ significantly all measured domain wall width were found to be independent of the specific sample. This is explained by the identical shape of the electrical field inside the sample which is the basis of our analytical model.

Acknowledgments

We thank L. Tian and V. Gopalan for fruitful discussions.

We thank G. Baldenberger from the Institut National d'Optique (Canada) for providing the PPLN samples, D. Rytz from the Forschungsinstitut für mineralische und metallische Werkstoffe (Germany) for providing the BaTiO₃ and KNbO₃ samples. Financial support of the DFG research unit 557 and of the Deutsche Telekom AG is gratefully acknowledged.

-
- [1] R. W. Eason, A. S. Boyland, S. Mailis, and P. G. R. Smith, *Opt. Commun.* **197**, 201(2001).
 - [2] M. M. Fejer, G. A. Magel, D. H. Jundt, and R. L. Byer, *IEEE J. Quantum Electron.* **28**, 2631 (1992).
 - [3] V. S. Ilchenko, A. A. Savchenkov, A. B. Matsko, and L. Maleki, *Phys. Rev. Lett.* **92**, 043903 (2004).
 - [4] N. G. R. Broderick, G. W. Ross, H. L. Offerhaus, D. J. Richardson, and D. C. Hanna, *Phys. Rev. Lett.* **84**, 4345 (2000).
 - [5] Y. Cho, S. Hashimoto, N. Odagawa, K. Tanaka, and Y. Hiranaga, *Appl. Phys. Lett.* **87**, 232907 (2005).
 - [6] J. Padilla, W. Zhong, and D. Vanderbilt, *Phys. Rev. B* **53**, R5969 (1996).
 - [7] B. Meyer and D. Vanderbilt, *Phys. Rev. B* **65**, 104111 (2002).
 - [8] G. Catalan, J. F. Scott, A. Schilling, and J. M. Gregg, *J. Phys.: Condens. Matter* **19**, 022201 (2007).
 - [9] T. J. Yang, V. Gopalan, P. J. Swart, and U. Mohideen, *Phys. Rev. Lett.* **82**, 4106 (1999).
 - [10] V. Dierolf, C. Sandmann, S. Kim, V. Gopalan, and K. Polgar, *J. Appl. Phys.* **93**, 2295 (2003).
 - [11] M. Foeth, A. Sfera, P. Stadelmann, and P.-A. Buffat, *J. Electron. Microsc.* **48**, 717 (1999).
 - [12] Y. Cho in *Ferroelectric Thin Films*, Topics Appl. Phys. **98**, 105 (2005) Springer (Berlin Heidelberg)
 - [13] R. E. Newnham, *Properties of Materials* (Oxford University Press, New York, 2005)
 - [14] M. Alexe and A. Gruverman, eds., *Nanoscale Characterisation of Ferroelectric Materials* (Springer, Berlin; New York, 2004) 1st ed.
 - [15] O. Kolosov, A. Gruverman, J. Hatano, K. Takahashi, and H. Tokumoto, *Phys. Rev. Lett.* **74**, 4309 (1995).
 - [16] T. Jungk, A. Hoffmann, and E. Soergel, *Appl. Phys. Lett.* **89**, 163507 (2006).
 - [17] T. Jungk, A. Hoffmann, and E. Soergel, *J. of Microsc.* accepted (2007).
 - [18] H. Allik and T. J. R. Hughes, *International Journal for Numerical Methods in Engineering* **2**, 151 (1970).
 - [19] L. Tian, P. Capek, S. Choudhury, E. A. Eliseev, A. N. Morozovska, V. Dierolf, L. Chen, S. Kalinin, and V. Gopalan, to be published
 - [20] W. Greiner, *Klassische Elektrodynamik*. Harri Deutsch Verlag, Frankfurt am Main, (2002).
 - [21] T. Jungk, A. Hoffmann, and E. Soergel, *cond-mat/0602137*
 - [22] B. J. Rodriguez, R. J. Nemanich, A. Kingon, A. Gruverman, S. V. Kalinin, K. Terabe, X. Y. Liu, and K. Kitamura, *Appl. Phys. Lett.* **86**, 012906 (2005).